

MONITORING THE REMOTE PRIMARY CLOCK BY USING GPS CARRIER PHASE

S.-S. Chen¹, H.-M Peng¹, and C.-S. Liao²

1. Associate Researcher, National Standard Time & Frequency Lab., TL,
Chunghwa Telecom Co., Ltd., Taiwan
2. Senior Researcher, National Standard Time & Frequency Lab., TL,
Chunghwa Telecom Co., Ltd., Taiwan

Telecommunication Laboratories Chunghwa Telecom Co., Ltd.
12, Lane 551, Min-Tsu Road Sec. 5 Yang-Mei, Taoyuan, Taiwan 326, R.O.C.
Tel: +886-3-4245245 Fax: +886-3-4245474
E-mail: berry@cht.com.tw

Abstract

TL has developed the new system for remote frequency calibrations by using the GPS carrier-phase observation. Remote sites can obtain the stability and accuracy of their frequency bases and the traceability to the TL frequency standard through the system. Since the GPS carrier-phase observation is more precise than the pseudorange measurement, we use it to estimate the frequency performance of a remote frequency source with respect to the TL frequency standard. Our system contains the master site installed at TL and the remote site installed at the customer. In the remote site, the signal from the remote frequency base is fed into the GPS receiver to replace its internal frequency. Hence, the frequency offset with respect to the GPS satellite clock can be obtained by performing the time difference (differences between two epochs) on carrier-phase observations. Under this circumstance, our system is able to monitor frequency performance at the real-time processing. At the master site, we set up the same GPS receiver at TL and performed the carrier-phase single difference (differences between two receivers at TL and the remote site) and time difference at the post processing. This extra system option can provide the traceability to TL and better system uncertainty. The data of remote sites can be sent to TL through the PSTN (Public Switched Telephone Network) or the Internet. We did some tests to verify the calibration system and the distance is about 270 km between the remote site and TL. In fact, the whole system is good to calibrate and monitor the frequency of the remote oscillator. The system stability is about $2 \cdot 10^{-11}$ per second and $6 \cdot 10^{-14}$ per day. Now, we have already installed the calibration system at the customers' sites, and provided calibration reports to them.

INTRODUCTION

The frequency source plays a key role in many applications, such as telecommunication networks, power systems, navigation systems, and instrumentation calibration systems, etc. According to the frequency stability requirements of these systems, the frequency calibration and monitoring are very important. There are many methods to calibrate the remote oscillators. For example, the GPSDO (GPS Disciplined Oscillator) [1] is a well-known system that has the traceability to the GPS frequency standard. In general, the GPSDO estimates phase differences between the local oscillator and the GPS frequency standard by

using the pseudorange observations. The system stability is about $4 \cdot 10^{-10}$ per second and $5 \cdot 10^{-13}$ per day. It has good long-term stability. However, the short-term stability of the system could not meet the requirement of real-time frequency monitoring because of the large frequency variation in the short-term [2].

Hence, we improved the GPSDO by using carrier-phase observations, because the time and frequency dissemination using GPS carrier phase have higher resolution than using pseudorange measurements. In our system, the remote sites estimate the frequency performance of the local frequency base with respect to the GPS frequency standard by using carrier-phase observations. The stand-alone system stability is about $2 \cdot 10^{-11}$ per second and $2 \cdot 10^{-13}$ per day. So the remote site using the carrier-phase observations can meet the requirement of real-time frequency monitoring and its long-term stability is good enough to calibrate the cesium clock. Additionally, at the master site, we set up the same GPS receiver at TL, and performed the carrier-phase single difference and time difference at the postprocessing. The data of the remote site can be sent to TL through the PSTN and the Internet. This extra system option can provide the traceability to TL and better system uncertainty because the tropospheric and ionospheric delay can be eliminated. Some tests show that the system stability can be improved to about $2 \cdot 10^{-11}$ per second and $6 \cdot 10^{-14}$ per day under the 270 km baseline.

This paper provides a brief introduction of the frequency monitoring. Then it describes the monitoring system delivered to the customer's site and how to use the GPS carrier phase in frequency calibrations. The frequency monitoring tests under the 270 km baseline between TL and the remote site are also presented.

THE MODEL OF GPS CARRIER-PHASE OBSERVABLES

The typical model of GPS carrier-phase observables [3], [4] is

$$\Phi_A^j = \rho_A^j + c(dt^j - dT_A) + \lambda N_A^j - d_{ion}^j + d_{trop}^j + \varepsilon_A^j \quad (1)$$

where Φ_A^j is the carrier-phase measurement of the receiver A from the j^{th} GPS satellite; ρ_A^j is the true distance between the receiver A and the j^{th} GPS satellite; c is the speed of light; dT_A represents the clock difference between the GPS time and receiver A clock; λ is the GPS carrier-phase wavelength; N_A^j denotes the initial phase integer ambiguity; and d_{ion}^j and d_{trop}^j are the ionospheric delay and the tropospheric delay, respectively; ε_A^j is the unmodeled errors primarily due to multipath, temperature variation, physical factors, etc. The unit of the phase observable Φ_A^j in the equation is meter. To study the frequency synchronization, we would like to first examine the behavior of the oscillator. Hence, the GPS receiver's internal clock will be replaced by an external one. Under this arrangement, the term dT_A in Equation (1) represents the time difference between the GPS clock and the external clock A.

In our system, the remote site performs the time difference (differences between two epochs) on carrier-phase observations to obtain the phase difference with respect to the GPS time. If the satellite signal is continuously tracked and there is no cycle slip occurring, the cycle ambiguities N_A^j remain a constant. The time difference equation is

$$\delta\Phi_A^j = \delta\rho_A^j + c\delta dt^j - c\delta dT_A - \delta d_{ion}^j + \delta d_{trop}^j + \delta\varepsilon_A^j \quad (2)$$

where $\delta(\cdot)$ denotes the operator for differences between two epochs. The δdT_A represents the phase difference with respect to the GPS system time. The unmodeled ionospheric delay δd_{ion}^j and tropospheric delay δd_{trop}^j cannot be eliminated and they are regarded as error of the frequency offset. On the other hand, the master site has the same GPS receiver and performs the time difference the same as the remote site. Additionally, the master site performs the single difference between two receivers at the postprocessing. Denoting the two receivers by A and B and the satellite by j, respectively, the time-difference and the single-difference equation is

$$\Delta\delta\Phi_{AB}^j = \Delta\delta\rho_{AB}^j - c\Delta\delta dT_{AB} + \Delta\delta\varepsilon_{AB}^j \quad (3)$$

where $\Delta(\cdot)$ represents the operator for differences between receivers with the same satellite. Due to the strong correlation between the unmodeled ionospheric and tropospheric delays of the two receivers in the local area, the terms d_{ion}^j and d_{trop}^j in (1) are then eliminated. Since dT_A and dT_B are both referring to the same GPS time, their difference $\Delta\delta dT_{AB}$ in (3) is the phase difference between external clock A and external clock B.

SYSTEM ARCHITECTURE

Figure 2 shows the functional block diagram of our system. It consists of the master station and the remote station. The remote site includes the DDS manufactured by NOVATECH, an Ashtech G12 GPS receiver, and an industrial PC. In order to estimate the offsets of remote clocks with respect to the master clock or the GPS system time, the remote clocks are connected to the respective GPS receivers. Hence, the original internal quartz oscillators in all receivers are replaced. With the help of the frequency synthesizer, i.e. the DDS (Direct Digital Synthesizer) manufactured by NOVATECH, the signal of the external clock can be appropriately converted and then supplied to the GPS receiver. The frequency offset of the remote clock with respect to the GPS time can be estimated by performing the time difference (i.e. (2)) on carrier-phase observations. Equation (2) can be further expressed as follows:

$$\delta\Phi_A^j - \delta\rho_A^j - c\delta d t^j = -c\delta d T_A - \delta d_{ion}^j + \delta d_{trop}^j + \delta\varepsilon_A^j \quad (4)$$

in which the left-hand side of the equation is the difference of measured data and known values. The coordinates of the GPS antenna are predetermined by IGS (International GPS Service), and the coordinates and the satellite clock error of the jth GPS satellites are obtained from the broadcast navigation message. However, the unmodeled ionospheric delay δd_{ion}^j , the tropospheric delay δd_{trop}^j and some noise errors affecting the estimation of the frequency offset may occur in the evaluation of the right-hand side. This term $\delta d T_A(t_i) (= \delta d T_A(t_i) - \delta d T_A(t_{i-1}))$, where $t_i = t_{i-1} + \tau$ can be obtained by averaging (4) for all in view GPS observations. As previously mentioned, since $\delta d T_A(t_i)$ is the phase difference between remote clock and the GPS time, the associated estimate frequency offset $\hat{y}_r(t_i)$ is

$$\hat{y}_r(t_i) = -\frac{\delta d T_A(t_i)}{\tau} + \frac{-\delta d_{ion}^j + \delta d_{trop}^j + \delta\varepsilon_A^j}{c\tau} \quad . \quad (5)$$

On the other hand, the master station contains the DDS, an Ashtech G12 GPS receiver, and an industrial PC which are the same as the remote site owns. The carrier-phase data and other GPS observations messages are passed from the remote sites through the PSTN or the Internet. The frequency offset of the

remote clock with respect to the master clock can be estimated by performing the time difference (i.e. (2)) and then single difference (i.e. (3)) on carrier-phase observations. In the process, the biases and errors from satellites and receivers can be significantly reduced. Equation (3) can be further expressed as follows:

$$\Delta\delta\Phi_{AB}^J - \Delta\delta\rho_{AB}^J = -c\Delta\delta dT_{AB} + \Delta\delta\varepsilon_{AB}^J \quad (6)$$

This term $\Delta\delta dT_{AB}(t_i)$ ($=\Delta\delta dT_{AB}(t_i) - \Delta\delta dT_{AB}(t_{i-1})$, where $t_i = t_{i-1} + \tau$) can be obtained by averaging (6) for all in view GPS observations. Then the associated estimate frequency offset $\hat{y}_r(t_i)$ is

$$\hat{y}_r(t_i) = -\frac{\Delta\delta dT_{AB}(t_i)}{\tau} + \frac{\Delta\delta\varepsilon_{AB}^J}{c\tau} \quad . \quad (7)$$

We can obtain the frequency stability and accuracy by performing (5) at the real-time processing and also by performing (7) at the postprocessing. At the real-time processing, the frequency performance can be obtained as soon as possible. At the postprocessing, the system has the traceability to TL and the ionospheric delay and tropospheric delay can be reduced by the single difference. So the whole system can monitor and calibrate the remote clock by using (5) and (7) at the same time.

EXPERIMENTAL RESULT

The basic experimental structure for tests is shown in Figure 2. The remote site was built at Kaohsiung, which is 270 kilometers from the master site built at TL. The frequency base at the remote site is an HP5071A cesium clock. Figure 3(a) shows that the stability analysis of the remote clock by using the stand-alone GPS pseudorange observations. The estimate can be regarded as the performance of the popular GPSDO. The system stability is about $4 \cdot 10^{-10}$ per second and $5 \cdot 10^{-13}$ per day. In our system, the stability analysis of the remote clock by using the stand-alone GPS carrier-phase observations is shown in Figure 3(b). The system stability is about $2 \cdot 10^{-11}$ per second and $2 \cdot 10^{-13}$ per day. Figure 3(c) shows that the stability analysis of the remote clock by using the postprocessing with the GPS carrier-phase observations of two sites. The system stability can be improved to about $2 \cdot 10^{-11}$ per second and $6 \cdot 10^{-14}$ per day under the 270 km baseline. In the test, we used the standard-performance cesium clock HP5071A and we tried to use it to evaluate the system uncertainty. In the stand-alone processing or the postprocessing, the whole system uncertainty contains the calibration uncertainty and the remote cesium clock uncertainty. For a conservative estimate, we took the whole test system uncertainty to be the class B uncertainty of the calibration system.

CONCLUSION

In this paper, a new scheme for frequency monitoring and calibration by using carrier-phase observations is presented. The customers can monitor their frequency bases through the stand-alone system. If they need the traceability and more accurate calibration reports, the postprocessing can meet the requirement. The tests show that the unmodeled ionospheric and tropospheric delays are strongly correlated within 270 km. And we can improve the system stability by postprocessing. Based on these results, we can provide a local calibration network within the distance of 270 km apart from TL. This situation is good to the Taiwan area. Potential applications of the system include the calibration of frequency sources in the telecommunication networks, secondary calibration laboratories, power systems, and others. We

have already installed one calibration system at the Chung-Shan Institute of Science and Technology (CSIST), and provided calibration reports to them.

ACKNOWLEDGMENTS

We gratefully acknowledge the NBS (National Bureau of Standards) of the R.O.C. for supporting this project.

REFERENCES

- [1] J. A. Davis and J. M. Furlong, 1997, "*Report on the study to determine the suitability of GPS disciplined oscillators as time and frequency standards traceable to the UK national time scale UTC(NPL)*," Centre for Time Metrology, National Physical Laboratory, UK.
- [2] F. Cordara and V. Pettiti, 1999, "*Short term characterization of GPS disciplined oscillators and field trial for frequency of Italian calibration centers*," in Proceedings of the 1999 Joint Meeting of the European Frequency and Time Forum (EFTF) and the IEEE International Frequency Control Symposium, 13-16 April 1999, Besançon, France (IEEE Publication 99CH36313), pp. 404-407.
- [3] B. Hofmann-Wellenhof, H. Lichtenegger, and J. Collins, 1994, **Global Positioning System: Theory and Practice** (Springer-Verlag, Vienna and New York).
- [4] D. Wells, 1996, **Guide to GPS Positioning** (Canadian GPS Associates).
- [5] G. Petit and C. Thomas, 1996, "*GPS frequency transfer using carrier-phase measurements*," in Proceedings of the 1996 IEEE Frequency Control Symposium, 5-7 June 1996, Honolulu, Hawaii, USA (IEEE Publication 96CH35935), pp. 1151-1159.
- [6] C. Bruyninx, P. Defraigne, J. M. Sleewaegen, and P. Paquet, 1999, "*Frequency transfer using GPS: comparative study of code and carrier phase analysis results*," in Proceedings of the 30th Precise Time and Time Interval (PTTI) Systems and Applications Meeting, 1-3 December 1998, Reston, Virginia, USA (U.S. Naval Observatory, Washington, DC), pp. 307-314.

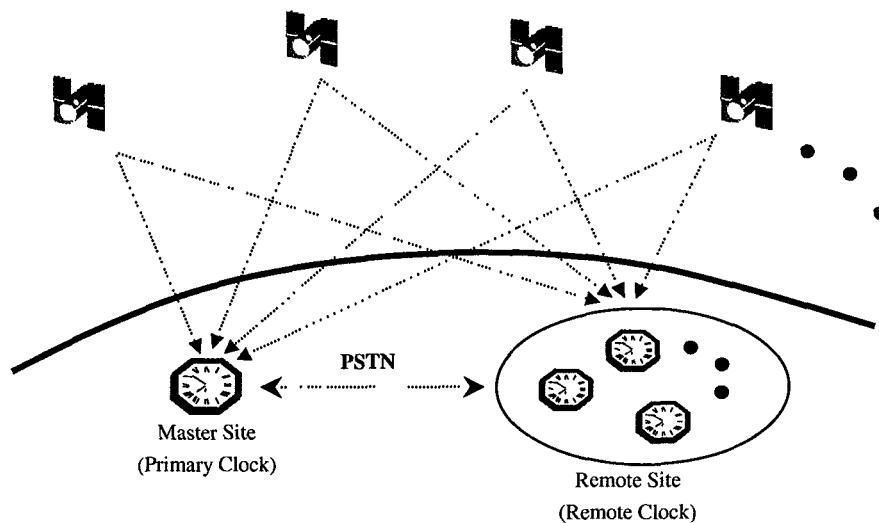


Figure 1. The basic architecture for the remote calibration by using GPS carrier-phase measurements.

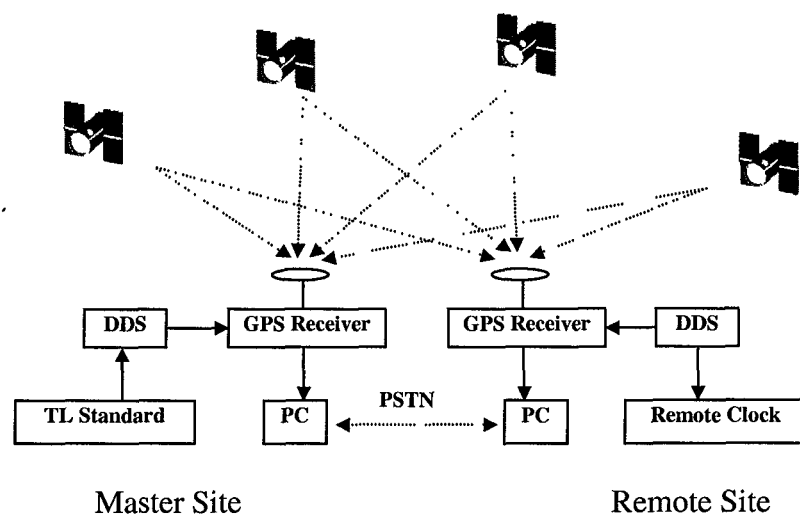


Figure 2. The block diagram for the frequency calibration using GPS carrier-phase measurements.

Frequency Stability

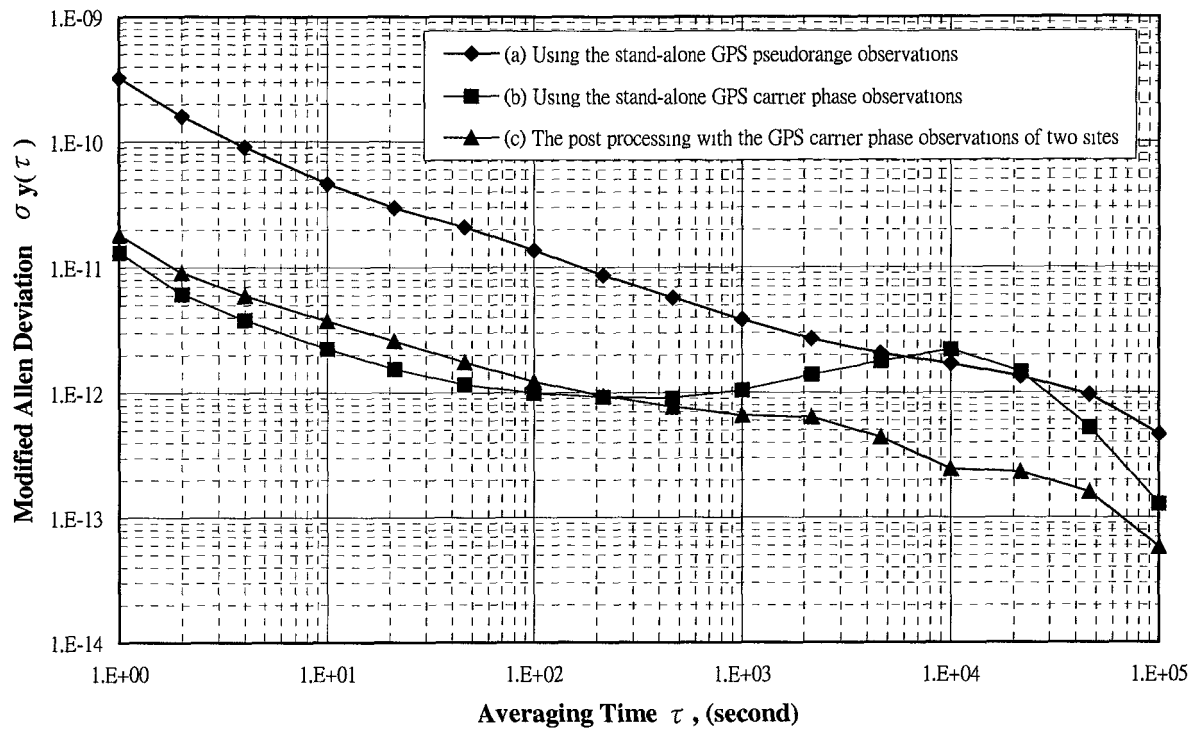


Figure 3. Systems stability analysis from the tests.